

Communication

Acetic Acid/Propionic Acid Conversion on Metal Doped Molybdenum Carbide Catalyst Beads for Catalytic Hot Gas Filtration

Mi Lu ^{1,†}, Andrew W. Lepore ^{2,†}, Jae-Soon Choi ¹, Zhenglong Li ¹, Zili Wu ²,
Felipe Polo-Garzon ² and Michael Z. Hu ^{1,*}

¹ Energy and Transportation Sciences Division, Oak Ridge National Laboratory, Oak Ridge, TN 37831, USA; lum1@ornl.gov (M.L.); choijs@ornl.gov (J.-S.C.); liz3@ornl.gov (Z.L.); hum1@ornl.gov (M.Z.H.)

² Chemical Science Division, Oak Ridge National Laboratory, Oak Ridge, TN 37830, USA; leporeaw@ornl.gov (A.W.L.); wuz1@ornl.gov (Z.W.); pologarzonf@ornl.gov (F.P.-G.)

* Correspondence: hum1@ornl.gov; Tel.: +865-574-8782

† These authors contributed equally to this work.

Received: 14 November 2018; Accepted: 7 December 2018; Published: 9 December 2018



Abstract: Catalytic hot gas filtration (CHGF) is used to precondition biomass derived fast pyrolysis (FP) vapors by physically removing reactive char and alkali particulates and chemically converting reactive oxygenates to species that are more easily upgraded during subsequent catalytic fast pyrolysis (CFP). Carboxylic acids, such as acetic acid and propionic acid, form during biomass fast pyrolysis and are recalcitrant to downstream catalytic vapor upgrading. This work developed and evaluated catalysts that can convert these acids to more upgradeable ketones at the laboratory scale. Selective catalytic conversion of these reactive oxygenates to more easily upgraded compounds can enhance bio-refinery processing economics through catalyst preservation by reduced coking from acid cracking, by preserving carbon efficiency, and through process intensification by coupling particulate removal with partial upgrading. Two metal-doped molybdenum carbide (Mo₂C) supported catalyst beads were synthesized and evaluated and their performance compared with an undoped Mo₂C control catalyst beads. For laboratory scale acetic acid conversion, calcium doped Mo₂C supported catalyst beads produced the highest yield of acetone at ~96% at 450 °C among undoped and Ca or Ni doped catalysts.

Keywords: bio-oil; biomass conversion; carbide catalyst; ketonization; doped carbides

1. Introduction

Hot gas filtration (HGF) can reduce alkali and alkaline earth metals and solid content from biomass fast pyrolysis vapors in order to improve vapor composition and protect downstream upgrading and hydrotreatment catalysts from fouling [1]. Packing the catalyst beads to the filter, which becomes catalytic hot gas filtration (CHGF), can further upgrade bio-oil vapor and provide chemical tailoring of the feed vapors before they enter the downstream upgrading. Among various bio-oil components, carboxylic acids, such as acetic acid and propionic acid, ~10 wt%, are commonly found in large amounts in bio-oils and contribute to the acidic and corrosive nature of bio-oil [2]. Furthermore, these acids are of low value and present challenges in downstream bio-oil upgrading processes. Small organic acids in liquid bio-oil can catalyze polymerization of reactive species, such as sugars and aldehydes, during hydroprocessing, cause catalyst fouling, and consume an excessive amount of H₂ producing low-value alkane hydrocarbon gases [3]. This laboratory scale study developed and evaluated catalysts targeting carboxylic acid and small carbonyl conversion to more upgradeable species.

Various reactions for carboxylic acids on metal or oxide catalysts have been well studied. For instance, hydrodeoxygenation (HDO) of acetic acid produces ethanol [4], decarboxylation (DCO) produces CO_2 [5], dehydration yields ethenone [5], reduction produces acetaldehyde [6], and ketonization leads to the production of acetone [7]. The selectivities for these reactions depend strongly on the nature of the catalyst surface. In general, HDO is an attractive route to upgrade bio-oil, considering that this process is well established in the petroleum industry; however, HDO of bio-oil usually requires precious metals, high temperatures, and high hydrogen pressures [8,9]. For example, Huber et al. used Ru/C and Pt/C catalysts to produce bi- and tri-cyclic products from phenol with 85% selectivity at 160 °C and 5 MPa hydrogen pressure [3]. The amount of precious metals needed for the degradation of cellulose was relatively high, 4–10 mg per gram of cellulose [9]. Moreover, precious metals have a greater tendency towards DCO over HDO and tend to fully saturate double bonds via hydrogenation. Therefore, it is desirable to develop inexpensive catalysts that can perform carboxylic acid conversion under mild conditions. Interstitial carbides are robust materials which have catalytic properties similar to those of precious metals due to their electronic structure [9]. On the other hand, carbides, such as Mo_2C , have been shown to be more selective towards HDO than DCO as well as have superior stability under upgrading conditions [10–12]. By being less active towards C-C bond scission, the hydrocarbons produced typically have greater molecular weight and value [10].

Most of the studies on Mo_2C focus on its direct hydrodeoxygenation properties. Very few reports show modifications of the crystal structure of molybdenum carbide to fine-tune its catalytic activity. We tested Ni- Mo_2C for bio-oil stabilization in our previous study [13]. In this study, we explored the ketonization activity for acetic and propionic acid conversion by modifying Mo_2C with Ca and Ni in catalyst beads form designed for CHGF. We found that we could tune the selectivity toward ketone production by doping Mo_2C with Ca. In-situ chemistry tailoring of hot pyrolysis vapors serves as an alternative processing method to process vapors before they are condensed into bio-oil liquid for more facile subsequent upgrading to hydrocarbon fuels and chemicals. Besides the filtration removal of inorganic mineral (alkali/alkaline metals), catalyst beads-loaded hot gas filters are being developed to enable selective target conversions (such as conversion of carboxylic acids and small carbonyls). Therefore, transforming these carboxylic acids/carbonyls into larger more upgraded molecules before condensation would be beneficial with respect to H and C economy and hydroprocessing catalyst lifetime.

2. Results and Discussion

Propionic acid conversion and product selectivity was dependent upon reaction temperature for all three Mo_2C catalysts (Figure 1A–C). Un-doped Mo_2C (Figure 1A) had three main products: C3 hydrocarbons (propane and propene), C2 hydrocarbons (ethane and ethylene), and propionaldehyde. At 250 °C, propionaldehyde was the major product (55% selectivity) indicating that hydrogenation was the dominant reaction pathway. The presence of C3 species were also significant at 35% selectivity. The propene could have come from dehydration of 1-propanol produced by propionaldehyde hydrogenation. It is known that Mo_2C surface can possess acidic sites due to the presence of surface oxygen [14]. 1-Propanol, however, was not detected throughout the experiment. This suggests that either 1-propanol dehydration was very fast (i.e., consumed as soon as it formed), or propene was produced by direct hydrogenolysis of the aldehyde carbonyl group [10]. C2 products, on the other hand, were negligible. This suggests that cracking or hydrogenolysis reactions were not predominant under these conditions. As the reaction temperature increased from 250 to 350 °C, the selectivity shifted away from propionaldehyde to C3 species. The olefin selectivity is the alkene selectivity over the sum of the alkane and alkene species. Propene was ~80% of the C3 products, indicating that the catalyst had moderate activity toward double bond hydrogenation under these conditions. A similar trend was observed with C2 species. Increasing the reaction temperature further to 450 °C drove the selectivity towards C2 species, with ethylene being the major fraction. One possible explanation for this transition is that C-C bond cleavage of propene molecules became a dominant reaction pathway

at high temperatures. However, considering the limited CH_4 formation, its reactivity towards C-C bond cleavage was still relatively modest compared to precious metal catalysts which would have produced predominantly CH_4 gas at this temperature. Reducing the temperature back down to 250 °C revealed that the catalyst's activity had significantly decreased over the experiment, evidenced by the low propionic acid conversion (~5%).

Nickel-doped Mo_2C (Figure 1B) was subjected to a slightly different reaction temperature scheme which was as follows: 250 → 350 → 450 °C. As in the case of un-doped Mo_2C , propionaldehyde was the major product. However, selectivity patterns as a function of temperature presented some substantial differences. This catalyst exhibited a dramatic increase in 3-pentanone at 450 °C as compared with the un-doped catalysts (25 vs. 2.5% selectivity, respectively). Interestingly, the 3-pentanone selectivity was much higher at 350 °C at the end of the experiment than it was in the beginning (15 vs. 1.5%, respectively). On the other hand, the C3 selectivity decreased from 30 to 3% over the course of the experiment. The olefin selectivity appeared unchanged. This suggests that as the catalyst became less active towards propionic acid hydrogenation and dehydration (and/or deoxygenation), the ketonization activity improved. Further investigation into the catalyst acidity and the mode of deactivation is necessary to understand the phenomena behind this mechanistic shift.

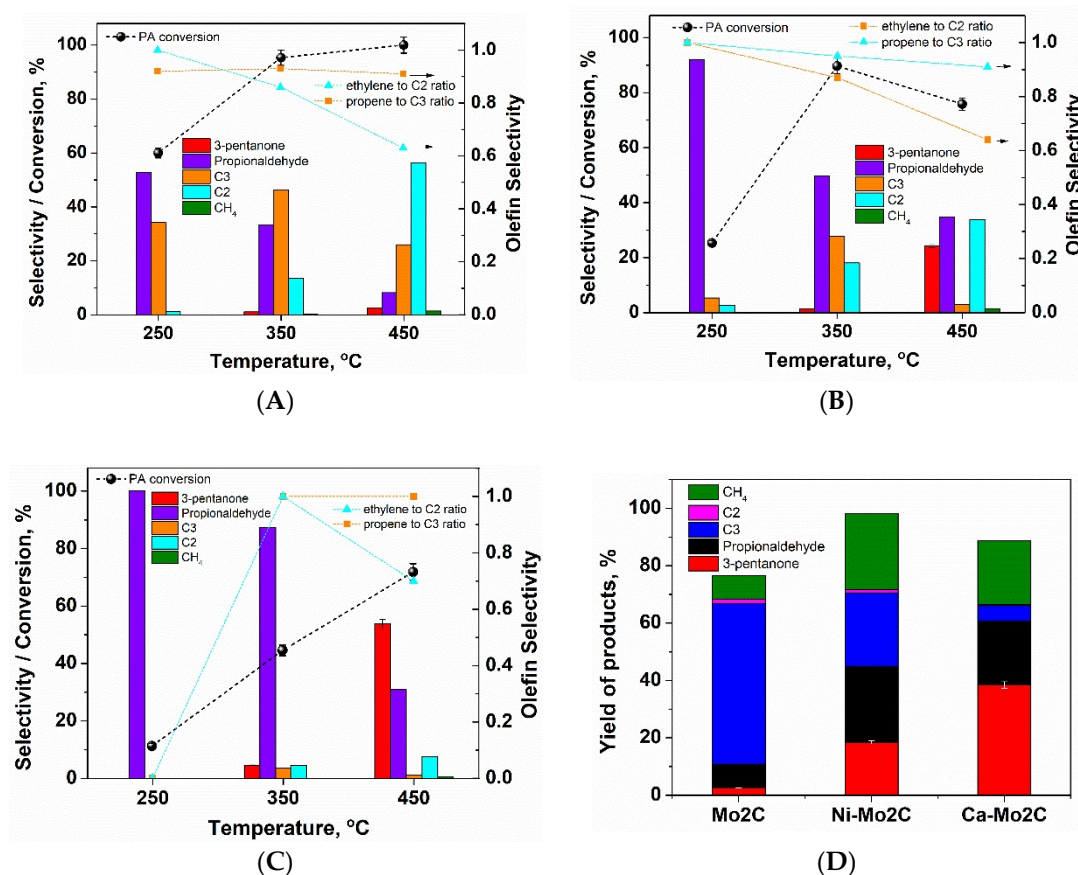


Figure 1. Product selectivity and propionic acid conversion over three types of carbide pellet catalysts after pretreatment with 10% H₂ at 500 °C for 2 h: (A) Mo₂C, 4 h time on stream (TOS); (B) Ni-Mo₂C, 4 h TOS; (C) Ca-Mo₂C, 4 h TOS, but the final injection was taken after running the reaction for 12 h; (D) yield of products at 450 °C over three types of carbide catalysts.

The Ca-doped Mo₂C was subjected to the following temperature scheme: 250 → 350 → 450 °C (Figure 2C). The behavior of the calcium doped Mo₂C was remarkably different from the un-doped and the nickel doped catalysts. At 250 °C, the catalyst was less active (acid conversion ~10%). However, increasing the reaction temperature improved acid conversion monotonously. At low temperatures,

propionaldehyde was again highly favored, but at elevated temperatures 3-pentanone was dominant. The C3 and C2 hydrocarbons remain minor byproducts over the entire temperature range. At 500 °C, 3-pentanone selectivity was 62% and propionic acid conversion was 96%. The reaction was continued at this temperature for 12 h, at which point the 3-pentanone selectivity increased to 83%, but the acid conversion had dropped to 45%. Therefore, the deactivation of Ca-Mo₂C was mainly accompanied by loss in its hydrogenation function while maintaining its ketonization selectivity.

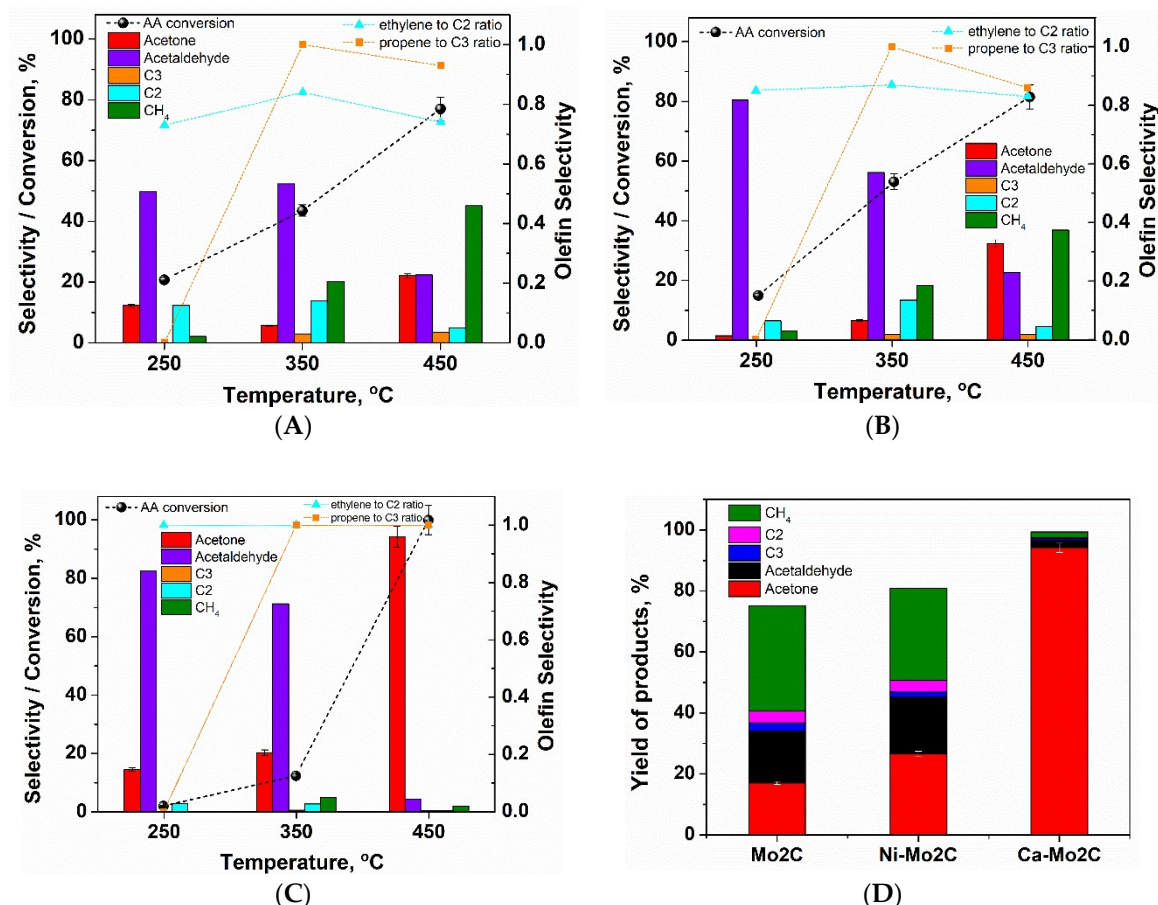


Figure 2. Product selectivity and acetic acid conversion over three types of carbide pellet catalysts after pretreatment with 10% H₂ at 500 °C for 2 h: (A) Mo₂C, 4 h TOS; (B) Ni-Mo₂C, 4 h TOS; (C) Ca-Mo₂C, 4 h TOS; (D) yield of products at 450 °C over three types of carbide catalysts.

In view of our results of propionic acid hydrodeoxygenation over metal carbides, we reasoned that acetic acid could go through ketonization to form acetone over metal carbides, as well. Hydrogenation of acetone can lead to 2-propanol which can subsequently be dehydrated to propene. Hydrodeoxygenation of acetic acid was carried out over un-doped, Ni-, and Ca-Mo₂C. Product selectivity and acid conversion as a function of reaction temperature are summarized in Figure 2A–C. Each reaction in this series was subjected to the same temperature sequence which was as follows: 250 → 350 → 450 °C. The only exception to this was Ca-Mo₂C's final temperature, which was 350 °C, because sampling at 250 °C would not have yielded useful data due to low conversion.

The un-doped catalyst produced mainly acetaldehyde at 250 °C, and the conversion was low (~20%) (Figure 2A). As the reaction temperature increased to 350 and 450 °C, the conversion improved. However, selectivity towards methane became dominant (45% at 450 °C) indicating increased contribution from the DCO pathway. Acetone, the ketonization product, was being produced over the un-doped carbide; however, the yield was only ~15% at 450 °C (Figure 2D).

Ni-doped Mo₂C had highest selectivity towards aldehyde product at 250 °C (Figure 2B). This was consistent with the results seen from propionic acid hydrodeoxygenation. At higher temperatures methane and acetone became major products, and the acetaldehyde selectivity was diminished similarly to the un-doped Mo₂C. Returning to the lower temperature again revealed that catalyst deactivation had also occurred to this catalyst. Acetone selectivity was yet again enhanced in the catalyst's less active state. As described below in the surface properties section the surface area and porosity of this catalyst did not experience any significant changes. The hydrogen activation property of carbides is known to suffer with surface oxygen accumulation, while oxygen-modified carbide surfaces present acid properties [15]. The observed deactivation could therefore be related to surface oxygen accumulation with time on stream (TOS) and temperature [14].

Ca-doped Mo₂C provided the highest acetone selectivity (Figure 2C). At 450 °C quantitative conversion was achieved with 94% selectivity towards the ketone. At lower temperatures acetaldehyde selectivity was dominant. Little selectivity towards light gases, including methane, was observed. Furthermore, the C2 and C3 products detected were purely alkene, as shown in the olefin selectivity. This suggests that Ca-Mo₂C was less active in reactions involving H₂ activation, such as acid hydrogenation, alkene hydrogenation, and hydrogenolysis. This property may arise from its “basic” nature. In one study looking at the decomposition of 2-propanol over Mo₂C, acetone selectivity was greatly enhanced by NH₃ poisoning [16,17]. This suggests that the basicity of the catalyst surface controls selectivity [16,17]. It has also been shown that both acid and basic sites exist on Mo₂C, and modification of these sites can have a profound effect on reactivity [18].

For better understanding the dopant effect on the acetic acid reactions, the total number of basic sites on three types of carbide catalysts were determined by temperature-programmed desorption of carbon dioxide (CO₂-TPD). The temperature for CO₂ desorption is usually an indication of the base site strength [18]. The amounts of CO₂ that desorbed from the carbide catalysts (Table 1) showed that Ca doped Mo₂C has the highest densities of basic sites (~1.77 micromoles/m²), which is more than double the amount for Mo₂C and Ni-Mo₂C. Our reaction data—Ca-Mo₂C showed the highest ketonization selectivity—suggests that basic sites were responsible for ketonization [19,20]. Previous work has shown that the doped Mo₂C synthesis method can have a dramatic effect on the physical and chemical properties of the catalyst [21]. The surface properties of the carbide catalysts both before and after reaction are also summarized in Table 1. Metal doping (which was done before carburization) had a significant effect on the surface area of the resulting catalyst. Among the fresh catalysts, the un-doped, Ni-doped, and Ca-doped catalysts had Brunauer-Emmett-Teller (BET) surface areas of 23.5, 18.3, and 9.6 m²/g, respectively. The addition of calcium had the greatest impact on surface area. It is believed that calcium slows the carburization process which leads to greater sintering, thus lowering the surface area [22]. The total pore volume followed a similar trend. The surface areas, post acetic acid hydrogenation, remained relatively unchanged; however, for Ca-Mo₂C, since we used the calcium alginate polymer type crosslink agent, it might have totally burned out during the high temperature reaction with acetic acid, thus the pore size was even larger after the reaction.

Table 1. Surface properties of three types of carbide catalysts.

Catalyst	^a CO ₂ Desorbed during TPD up to 550 °C, micromoles/m ²	Surface Area, m ² /g	Surface Area after Reaction *, m ² /g	Total Pore Volume, cm ³ /g	Total Pore Volume after Reaction *, cm ³ /g	Average Pore Size, Å	Average Pore Size after Reaction *, Å
Mo ₂ C	0.86	23.5	23.7	0.0925	0.0869	77.2	73.5
Ni-Mo ₂ C	0.79	18.3	17.2	0.0779	0.0701	85.2	81.4
Ca-Mo ₂ C	1.77	9.6	7.1	0.0375	0.0346	78.5	97.0

a: Temperature-programmed desorption of carbon dioxide (CO₂-TPD); * Post reaction with acetic acid.

3. Materials and Methods

The propionic acid ($\geq 99.5\%$), acetic acid ($>99\%$), CaCl_2 , and NiCl_2 were purchased from Sigma-Aldrich (St. Louis, MO, USA) and used as received. CH_4 (99.99%) and H_2 (99.999%) were purchased from AirGas (Radnor Township, PA, USA); MoO_3 and ammonium heptamolybdate powders were purchased from Alfa Aesar (Ward Hill, MA, USA).

3.1. Catalyst Synthesis and Characterization

3.1.1. Carbide Catalysts Beads Synthesis

The bulk Mo_2C catalysts used in this chapter were synthesized via the temperature-programmed carburization (TPC) described previously [23]. The undoped Mo_2C was prepared using pressure-pelletized heptamolybdate. To study the effects of metal doping on molybdenum carbide properties, metal doped MoO_3 precursors were prepared before carburization. The precursors were prepared via a gelation method [24]. In brief, MoO_3 powder was suspended in an aqueous solution of sodium alginate. The oxide slurry was dropped into an aqueous solution of a metal chloride (CaCl_2 or NiCl_2). The Na^+ ions in the alginate binder exchanged with the divalent metal ions (e.g., one Ca^{2+} ion for two Na^+ ions) causing the alginate polymer molecules to cross-link. This process created a rigid MoO_3 bead.

The precipitated oxide beads were separated from solution, rinsed, dried, and heat-treated at 600°C for 2 h in air. Alginate was removed by calcining the particle, leaving behind the doped MoO_3 beads. Carburization was accomplished via the TPC method in a tubular quartz reactor of ~ 2.5 cm internal diameter. During carburization, the oxygen was removed from molybdenum in the form of water and carbon monoxide, leaving behind Mo_2C . The carburizing gas consisted of 15% CH_4 and 85% H_2 (flow rate: 104 sccm per gram of precursor); the sample temperature was raised from room temperature to 700°C at $1^\circ\text{C}/\text{min}$ and held for 1 h. After cooling to room temperature, the synthesized carbides were passivated in a 1% O_2/N_2 flow for 12 h [25].

3.1.2. Specific Surface Area and Pore Size Analysis (BET)

The morphology of carbides was analyzed via N_2 sorption using a Quantachrome Autosorb-1. The samples were outgassed for 24 h at 400°C prior to analysis. The total pore volume was measured ($p/p_0 = 0.99$) using the Barrett-Joyner-Halenda (BJH) method. The pore size distribution was found using 19 point adsorption and 19 point desorption isotherms. The surface area was calculated from adsorption points with $p/p_0 < 0.35$ per the Brunauer-Emmett-Teller (BET) method.

3.1.3. Temperature Programmed Desorption of Carbon Dioxide (CO_2 -TPD)

An Altamira AMI-200 characterization instrument was used for the measurements. The samples were pretreated under 50 mL/min of 4% H_2/Ar for 3 h at approximately 500°C , and then flushed in 50 mL/min of Ar for 30 min at the same temperature. Afterwards, the sample was cooled down to 30°C under 50 mL/min of argon. Once at 30°C , 45 mL/min of 2% CO_2/Ar were flowed through the sample for 1 h. The gas flowing through the sample was switched to 45 mL/min of argon, and 1 h was allowed for weakly bound CO_2 species to desorb before the temperature programmed desorption (TPD) experiment was started. For the TPD experiment, 45 mL/min of argon were used as the carrier gas. The temperature was ramped from 30°C to 1000°C at a rate of $10^\circ\text{C}/\text{min}$, and then held at 1000°C for 1 h. The desorbed CO_2 was analyzed using a mass spectrometer.

3.2. Catalyst Testing

Acid hydrodeoxygenation experiments were conducted using a bench-top flow through reactor system. The product selectivity and reactant conversion were measured as a function of temperature and time on stream (TOS). These experiments were run under atmospheric pressure. In a typical test,

400 mg of catalyst was packed in a 1 cm I.D. quartz tube. After loading the catalyst, the bed was heated to 500 °C at a rate of 5 °C/min under 45 sccm helium. At 500 °C, 5 sccm H₂ was added to the helium stream. The pretreatment was continued for 2 h before cooling the reactor to a desired reaction temperature (e.g., 250 or 350 °C) at a rate of ~10 °C/min. The carboxylic acid was introduced into the reactor by redirecting H₂-He gas through a bubbler/saturator with an average flow of 0.15 mL/h, affording an effective space velocity of 0.37 h⁻¹ WHSV (acid basis). The exit vapor was analyzed by directly injecting into either the GC-FID (Agilent 7820A) for product quantification or GC-MS (Agilent 7890C GC/5975C MS) for product identification. Liquid product analysis was done with a gas chromatograph employing a HP-Plot Q capillary column (dimensions of 30.0 m × 320 µm × 20.0 µm) and an FID detector. For analysis, GC was held at 50 °C for 3 min, ramped up to 250 °C at 15 °C/min, and then held at that temperature for 20 min. A constant pressure mode of 9.51 psi was used, and the inlet temperature was 250 °C. After the first injection, the reactor temperature was increased and allowed to equilibrate for an hour. This was again repeated, and after the third injection the reactor was cooled to the initial temperature. Another sample was taken after an hour of equilibration. The fourth injection was meant to assess the stability of the material over the 4 h of operation. All the data were repeated at least three times to make sure the error was less than 3%.

4. Conclusions

We have shown that un-doped Mo₂C is active towards both acetic and propionic acid hydrodeoxygenation under atmospheric pressure. Additionally, we found that doping the MoO₃ with Ni or Ca prior to carburization can have dramatic effects on the physical characteristics as well as the reactivity of the resulting carbides. Ni-Mo₂C was found to be more active towards hydrogenation than the other catalysts. Ca-Mo₂C was found to exhibit superior selectivity (94%) for the acetone production, especially at high temperatures relevant to pyrolysis vapor upgrading, e.g., 450 °C. Overall, the reactivity trends observed on a given catalyst type were consistent between acetic and propionic acids. Thus, carbide catalysts appear promising for deoxygenation of bio-derived compounds, with the possibility of tailoring product selectivity via metal doping. In future studies, further catalyst testing on real past pyrolysis vapor and characterization would be useful for understanding the reaction pathways and would provide insight into the nature of the various active sites. This information would aid in tuning the physical and chemical properties of these materials to achieve greater conversions, enhanced selectivity, and extended durability.

Author Contributions: M.L., A.L., J.-S.C., and M.Z.H. conceived and designed the experiments; M.L. and A.L. performed the experiments; M.L., and A.L. analyzed the data; Z.L., Z.W., and F.P.-G. contributed during experiments and discussion; M.L. and A.L. wrote the paper with contribution from the other co-authors.

Funding: This research was funded by [Bioenergy Technology Office (BETO) of the Department of Energy (DOE)] grant number [WBS2.5.5.507] with Oak Ridge National Laboratory.

Acknowledgments: Beth Armstrong at Oak Ridge National Laboratory for help with the doped MoO₃ beads synthesis.

Conflicts of Interest: The authors declare no conflict of interest.

References

1. Baldwin, R.M.; Feik, C.J. Bio-oil stabilization and upgrading by hot gas filtration. *Energy and Fuels* **2013**, *27*, 3224–3238. [[CrossRef](#)]
2. Wang, H.; Male, J.; Wang, Y. Recent advances in hydrotreating of pyrolysis bio-oil and its oxygen-containing model compounds. *ACS Catal.* **2013**, *3*, 1047–1070. [[CrossRef](#)]
3. Huber, G.W.; Corma, A. Synergies between bio- and oil refineries for the production of fuels from biomass. *Angew. Chemie - Int. Ed.* **2007**, *46*, 7184–7201. [[CrossRef](#)] [[PubMed](#)]
4. Pallassana, V.; Neurock, M. Reaction paths in the hydrogenolysis of acetic acid to ethanol over Pd(111), Re(0001), and PdRe alloys. *J. Catal.* **2002**, *209*, 289–305. [[CrossRef](#)]

5. Nguyen, M.T.; Sengupta, D.; Raspoet, G.; Vanquickenborne, L.G. Theoretical study of the thermal decomposition of acetic acid: Decarboxylation versus dehydration. *J. Phys. Chem.* **1995**, *99*, 11883–11888. [[CrossRef](#)]
6. Pestman, R.; Koster, R.M.; Van Duijne, A.; Pieterse, J.A.Z.; Ponc, V. Reactions of carboxylic acids on oxides: 2. Bimolecular reaction of aliphatic acids to ketones. *J. Catal.* **1997**, *168*, 265–272. [[CrossRef](#)]
7. Martinez, R.; Huff, M.C.; Barteau, M.A. Ketonization of acetic acid on titania-functionalized silica monoliths. *J. Catal.* **2004**, *222*, 404–409. [[CrossRef](#)]
8. He, D.H.; Wakasa, N.; Fuchikami, T. Hydrogenation of carboxylic acids using bimetallic catalysts consisting of group 8 to 10, and group 6 or 7 metals. *Tetrahedron Lett.* **1995**, *36*, 1059–1062. [[CrossRef](#)]
9. Ji, N.; Zhang, T.; Zheng, M.; Wang, A.; Wang, H.; Wang, X.; Chen, J.G. Direct catalytic conversion of cellulose into ethylene glycol using nickel-promoted tungsten carbide catalysts. *Angew. Chemie - Int. Ed.* **2008**, *47*, 8510–8513. [[CrossRef](#)]
10. Ren, H.; Yu, W.; Saliccioli, M.; Chen, Y.; Huang, Y.; Xiong, K.; Vlachos, D.G.; Chen, J.G. Selective hydrodeoxygenation of biomass-derived oxygenates to unsaturated hydrocarbons using molybdenum carbide catalysts. *ChemSusChem* **2013**, *6*, 798–801. [[CrossRef](#)]
11. Xiong, K.; Yu, W.; Vlachos, D.G.; Chen, J.G. Reaction pathways of biomass-derived oxygenates over metals and carbides: From model surfaces to supported catalysts. *ChemCatChem* **2015**, *7*, 1402–1421. [[CrossRef](#)]
12. Jongorius, A.L.; Gosselink, R.W.; Dijkstra, J.; Bitter, J.H.; Bruijninx, P.C.A.; Weckhuysen, B.M. Carbon nanofiber supported transition-metal carbide catalysts for the hydrodeoxygenation of guaiacol. *ChemCatChem* **2013**, *5*, 2964–2972. [[CrossRef](#)]
13. Li, Z.; Choi, J.-S.; Wang, H.; Lepore, A.W.; Connatser, R.M.; Lewis, S.A.; Meyer, H.M.; Santosa, D.M.; Zacher, A.H. Sulfur-Tolerant Molybdenum Carbide Catalysts Enabling Low-Temperature Stabilization of Fast Pyrolysis Bio-oil. *Energy & Fuels* **2017**, *31*, 9585–9594.
14. Sullivan, M.M.; Chen, C.J.; Bhan, A. Catalytic deoxygenation on transition metal carbide catalysts. *Catal. Sci. Technol.* **2016**, *6*, 602–616. [[CrossRef](#)]
15. Sullivan, M.M.; Bhan, A. Acetone Hydrodeoxygenation over Bifunctional Metallic-Acidic Molybdenum Carbide Catalysts. *ACS Catal.* **2016**, *6*, 1145–1152. [[CrossRef](#)]
16. Bej, S.K.; Bennett, C.A.; Thompson, L.T. Acid and base characteristics of molybdenum carbide catalysts. *Appl. Catal. A Gen.* **2003**, *250*, 197–208. [[CrossRef](#)]
17. Bej, S.K.; Thompson, L.T. Acetone condensation over molybdenum nitride and carbide catalysts. *Appl. Catal. A Gen.* **2004**, *264*, 141–150. [[CrossRef](#)]
18. Hattori, H. Heterogeneous Basic Catalysis. *Chem. Rev.* **1995**, *95*, 537–558. [[CrossRef](#)]
19. Hendren, T.S.; Dooley, K.M. Kinetics of catalyzed acid/acid and acid/aldehyde condensation reactions to non-symmetric ketones. *Catal. Today* **2003**, *85*, 333–351. [[CrossRef](#)]
20. Mante, O.D.; Rodriguez, J. a.; Senanayake, S.D.; Babu, S.P. Catalytic conversion of biomass pyrolysis vapors into hydrocarbon fuel precursors. *Green Chem.* **2015**, *17*, 2362–2368. [[CrossRef](#)]
21. Han, J.; Duan, J.; Chen, P.; Lou, H.; Zheng, X.; Hong, H. Carbon-supported molybdenum carbide catalysts for the conversion of vegetable oils. *ChemSusChem* **2012**, *5*, 727–733. [[CrossRef](#)] [[PubMed](#)]
22. Jung, K.T.; Kim, W.B.; Rhee, C.H.; Lee, J.S. Effects of Transition Metal Addition on the Solid-State Transformation of Molybdenum Trioxide to Molybdenum Carbides. *Chem. Mater.* **2004**, *16*, 307–314. [[CrossRef](#)]
23. Lee, J.S.; Oyama, S.T.; Boudart, M. Molybdenum carbide catalysts. I Synthesis of unsupported powders. *J. Catal.* **1987**, *106*, 125–133. [[CrossRef](#)]
24. Lundberg, D. Flow Conditioners. *Control Eng.* **2006**, *53*, 2–7.
25. Choi, J.S.; Zacher, A.H.; Wang, H.; Olarte, M.V.; Armstrong, B.L.; Meyer, H.M.; Soykal, I.I.; Schwartz, V. Molybdenum Carbides, Active and in Situ Regenerable Catalysts in Hydroprocessing of Fast Pyrolysis Bio-Oil. *Energy and Fuels* **2016**, *30*, 5016–5026. [[CrossRef](#)]

